Tellus (2007), 59B, 338–349
Printed in Singapore. All rights reserved

TELLUS

The effects of biomass burning aerosols and clouds on the CO_2 flux in Amazonia

By PAULO H. F. OLIVEIRA[1]*, PAULO ARTAXO[1], CARLOS PIRES[1], SILVIA DE LUCCA[1], ALINE PROCÓPIO[2], BRENT HOLBEN[3], JOEL SCHAFER[3], LUIZ F. CARDOSO[4], STEVEN C. WOFSY[5] and HUMBERTO R. ROCHA[6], [1]*LFA – Laboratório de Física Atmosférica, Instituto de Física, Universidade de São Paulo, Rua do Matão, Travessa R, 187, São Paulo, SP, CEP 05508-900, Brazil;* [2]*Departamento de Engenharia Bioquímica, Universidade Federal do Rio de Janeiro, Av. Brig. Trompowski, Rio de Janeiro, R.J., CEP: 21949-900, Brazil;* [3]*NASA Goddard Space Flight Center, Greenbelt, United States.;* [4]*UNIR Fundação Universidade Federal de Rondônia, Campus de Ji-Paraná, Ji-Paraná, Brazil;* [5]*Harvard University, Department of Earth and Planetary Science, 29 Oxford St., Cambridge, MA 02138, USA;* [6]*Departamento de Ciências Atmosféricas – IAG - Universidade de São Paulo, Rua do Matão, 1226 - CEP 05508-900, São Paulo, SP - Brazil*

(Manuscript received 30 april 2006; in final form 28 December 2006)

ABSTRACT

Aerosol particles associated with biomass burning emissions affect the surface radiative budget and net ecosystem exchange (NEE) over large areas in Amazonia during the dry season. We analysed CO_2 fluxes as a function of aerosol loading for two forest sites in Amazonia as part of the LBA experiment. Aerosol optical thickness (AOT) measurements were made with AERONET sun photometers, and CO_2 flux measurements were determined by eddy-correlation.

The enhancement of the NEE varied with different aerosol loading, as well as cloud cover, solar elevation angles and other parameters. The AOT value with the strongest effect on the NEE in the FLONA-Tapajós site was 1.7, with an enhancement of the NEE of 11% compared with clear-sky conditions. In the RBJ site, the strongest effect was for AOT of 1.6 with an enhancement of 18% in the NEE. For values of AOT lager than 2.7, strong reduction on the NEE was observed due to the reduction in the total solar radiation. The enhancement in the NEE is attributed to the increase of diffuse versus direct solar radiation. Due to the fact that aerosols from biomass burning are present in most tropical areas, its effects on the global carbon budget could also be significant.

1. Introduction

Global emissions from fossil fuel burning have added large quantities of CO_2 to the atmosphere since the beginning of the last century (Schimel, 1995), and a variety of studies have examined the processes that could account for the fate of this additional carbon injected to the atmosphere, in both oceanic and terrestrial component of the global carbon cycle (e.g. Fan et al., 1998; Houghton et al., 2000). The tropical rain forest biome plays a large role in the global carbon budget (Melillo et al., 1996; Field et al., 1998), but there is great uncertainty about their current and future impact on atmospheric CO_2 concentrations (Tans and White 1998; Schimel et al., 2001).

Tropical forests in Amazonia play an especially important role in the terrestrial component of the global carbon cycle (Malhi et al., 1998; Kruijt et al., 2004), and they respond strongly to climate variability, such as changes in precipitation (Marengo et al., 2001), temperature and radiation (Procopio et al., 2004). Carbon cycling in Amazonia has been studied in several short and long term measurements, showing very different values for the CO_2 fluxes measured through the eddy-correlation technique (Grace et al., 1996; Malhi et al., 1998; Keller et al., 2001; Andreae et al., 2002; von Randow et al., 2002; Kruijt et al., 2004; Ometto et al., 2005). The first measurements of ecosystem CO_2 exchange conducted in Amazonia using eddy-correlation (Grace et al., 1995a,b, 1996; Malhi et al., 1998), suggested a huge net carbon uptake of 3–6 tC ha^{-1} yr^{-1}. The main problem with these measurements lie in the difficult in assessing the night time fluxes under stable conditions (von Randow et al., 2002; Kruijt et al., 2004; Ometto et al., 2005) that can cause large errors in the estimation of diurnal and annual carbon fluxes in tropical forests. Saleska et al. showed that forest disturbances also play a large role in carbon exchange at least for some areas in Amazonia (Saleska et al., 2003). In terms of carbon fluxes the

*Corresponding author.
e-mail: pauloh@if.usp.br
DOI: 10.1111/j.1600-0889.2007.00270.x

compilation of Ometto et al. (2005), indicates that in Amazonia the natural forest could be a small carbon sink of the order of -0.5 tC ha^{-1} yr^{-1}. These values are confirmed by dendometry measurements. Ometto indicates that the overall estimates from losses from deforestation and the assimilation by the natural forest in Amazonia showed a carbon flux range that goes from -3.0 to $+0.75$ PgC yr^{-1}.

Deforestation in the Amazon region, which has the largest continuous area of tropical forest, has been studied using remote sensing techniques (Fearnside et al., 1996). The average deforestation rate for the nineties was 17 000 km^2 per year, increasing to approximately 25 000 km^2 in 2002 and 2003 (INPE, 2004). Up to 2005, an estimated area of 16% of the total Brazilian Amazon area of 5.8 million km^2 have been deforested (INPE, 2004). Most of this process has been concentrated in the Southern and Eastern part of Amazonia, while the central areas, less accessible, are relatively preserved. Deforestation affects the ecosystem in several ways, first there is a change in the energy and water balance when forest is replaced by pastures and this change has the potential to alter the atmospheric water content and precipitation patterns (Silva Dias et al., 2002). Second, a large amount of aerosol particles is released to the atmosphere as forests are cut and burned in the course of managing pastures and fields, leading to profound changes in the atmospheric composition (Artaxo et al., 1998, 2002), surface radiation balance (Schafer et al., 2002a,b; Procopio et al., 2003, 2004), as well as in cloud cover due to the presence of large amounts of black carbon particles (Koren et al., 2004; Kaufman and Koren, 2006).

During biomass burning events in Amazonia, ground level particle concentrations of up to 800 μg m^{-3} have been observed (e.g. in Alta Floresta, north of Mato Grosso state). Aerosol optical thicknesses (AOT) of more than 3 at 500 nm are frequently observed. AOT is a measurement of the amount of aerosol particles integrated over the atmospheric column, weighted by the scattering and absorption properties of the average aerosol. It is defined mathematically as the integration of the *linear extinction coefficient* throughout the atmospheric column (Eck et al., 1998; Holben et al., 1998).

Particle number concentrations that are very low in the wet season, averaging around 300 particles per cubic centimetre, can reach very high concentrations of around 30 000 particles per cubic centimetre in the dry season (Andreae et al., 2002; Artaxo et al., 2002; Procopio et al., 2004). The interaction of the downward solar radiation with these particles and with clouds in the region, directly affect the atmospheric radiative budget, reducing the direct beam of downward solar radiation and increasing the diffuse fraction, especially in the wavelengths of the photosynthetically active radiation (PAR) region (Gu et al., 1999; 2003; Schafer et al., 2002a,b; Niyogi et al., 2004). The instantaneous reduction in total surface solar radiation can be as much as 375 Wm^{-2} (Schafer et al., 2002b) for PAR, and average daily values reduced by up to 37% (Procopio et al., 2004). The effects of this strong radiation deficit on the CO_2 net flux (net ecosystem exchange-NEE), and on the environmental variables that influence these CO_2 flux in the Amazonia, are complex and far from being fully understood. This large amount of aerosol can reduce surface temperatures by 2–3° degrees over large areas. Additionally, high atmospheric aerosol loading also changes cloud microphysics and low cloud occurrence that affects precipitation and surface radiation balance in significant ways (Andreae et al., 2004; Koren et al., 2004).

Field measurements in several different sites have showed that high CO_2 exchange occurs more frequently on cloudy days instead of clear-sky days (Price and Black, 1990; Hollinger et al., 1994; Gu et al., 1999, 2003; Niyogi et al., 2004). Some studies have showed that for a certain level of irradiance, cloudy days show higher NEE values compared with clear-sky days (Fan et al., 1995; Baldocchi, 1997; Niyogi et al., 2004). To explain such observations, some mechanisms have been postulated by various authors. They include an increase in the diffuse radiation fraction (Price and Black, 1990; Hollinger et al., 1994), a reduction in the vapour pressure deficit (VPD), and therefore a reduction of the respiration of tree leaves (Baldocchi, 1997), and other effects.

The major objectives in the present study are to quantify the influence of aerosol particles emitted by biomass burning on the NEE for two sites in Amazonia. We also want to analyse the net effect of the increase in the diffuse radiation fraction and the reduction of the total solar flux on carbon fluxes. Using long-term eddy-correlation flux data, plus meteorological and aerosol optical thickness measurements, this work presents strong evidence that the presence of aerosol particles can actually enhance CO_2 uptake in Amazonian forests sites during the dry season.

2. Site descriptions

Two LBA tower sites were chosen for this study; both have long term data for carbon fluxes and for aerosols and radiation. They are about 3000 km apart, with different climatology for precipitation and different biomass burning impacts. The Rondônia state site (Reserva Biológica Jarú-RBJ) is heavily influenced by biomass burning particles (Silva Dias et al., 2002; Andreae et al., 2004), and previous studies have shown high carbon assimilation for measurements at this site (von Randow et al., 2002). A second site in the Pará state (Floresta Nacional do Tapajós - FLONA-Tapajós), was chosen because of a smaller impact by biomass burning particles during dry season. FLONA-Tapajós is the only LBA site that shows net carbon loss overall from the ecosystem (Saleska et al., 2003). Figure 1 shows a map with the location of the two sites.

2.1. Reserva Biológica Jarú (RBJ)

The Reserva Biológica Jarú (RBJ) Tower Site (10°05′S and 61°55′W) is located approximately 100 km to the North of the urban area of Ji-Paraná, Rondônia, Brazil (Fig. 1). The RBJ

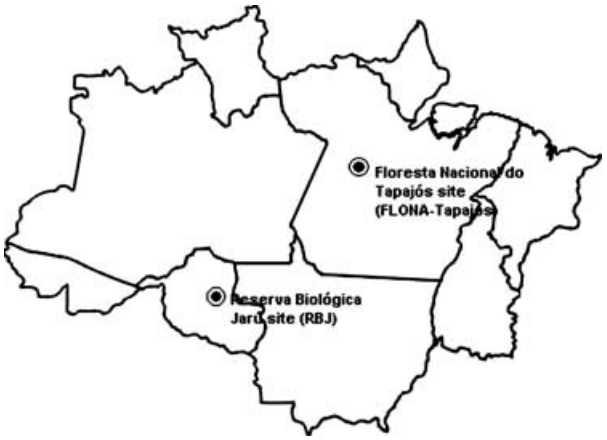

Fig. 1. Map of the sites studied: Reserva Biológica Jarú (RBJ), in Rondônia, Brazil and Floresta Nacional do Tapajós (FLONA-Tapajós), in Pará, Brazil.

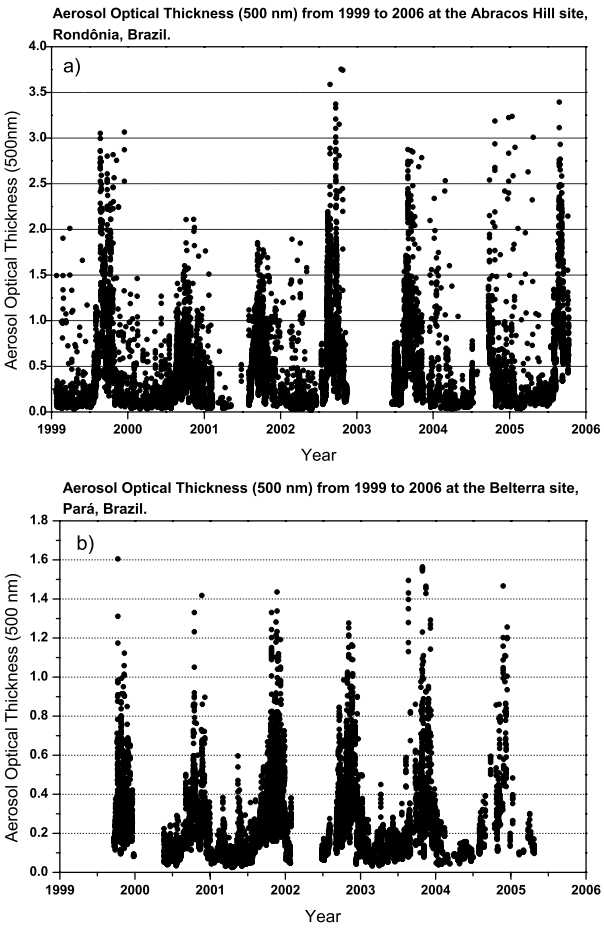

Fig. 2. Time series of aerosol optical thickness (AOT) at 500 nm from 1999 to 2006 for Abracos Hill site (a), in Rondônia, and for Belterra (b) site, in Pará, showing very high AOT values during the dry season.

is a 'terra firme' forest area with approximately 268 000 ha of undisturbed tropical forest, at an altitude varying between 100 and 150 m above mean sea level. The forest canopy has an average height between 30 and 35 m; however some trees can reach 45 m. Among the large number of different species that can be found at the RBJ are *Hymenaea courbaril* (Jatobá), *Apeiba tibourbou* (Pente de Macaco) and *Soracea guilleminiana* (Jaca-branca, Jaca-brava). The *Hymenaea* and *Apeiba* trees lose their leaves in the dry season, while the *Soracea* is an evergreen species.

The average temperature is almost constant throughout the year, but precipitation varies strongly with seasons. The southern hemisphere summer is the rainiest period in the region, with monthly totals over 200 mm. In contrast, during the dry season, from June to October, it is common to observe several weeks without rain. After the construction of the Cuiabá-Porto Velho highway (BR 364) in 1968, a dense network of adjacent roads to this highway gradually was built and the state is severely affected by deforestation. The area where the measurements were done is a protected area by Instituto Brasileiro do Meio Ambiente e dos Recursos Naturais Renováveis (IBAMA) and remains undisturbed over most of the area.

Figure 2a shows the time series of the aerosol optical thickness (500 nm) at the Abracos Hill site, near to Ji-Paraná, Rondônia, measured by the AERONET sun photometer from 1999 to 2006. Note the very high AOT values during the dry season due to biomass burning emissions. The wet season background AOT values are very low, on the order of 0.05.

2.2. *Floresta Nacional do Tapajós (FLONA-Tapajós)*

The FLONA-Tapajós Tower Site (3°01′S and 54°58′W) is located approximately 83 km to the south of Santarem city, in the Pará state, Brazil (Fig. 1). FLONA-Tapajós has an area of approximately 600 000 hectares characterized by dense primary forest on flat upland terrain, with an average canopy height between 35 and 40 m. The forest is semi deciduous, with mostly evergreen and a few deciduous species. Among the dominant species are *Cedrela odorata* (Cedar), *Aniba guianesis* (Blond), *Lecythis pisonis* (Chestnut sapucaia) and *Mezelaurus itaúba* (Itaúba), among others.

The FLONA-Tapajós dry season, which extends from August to November, are the months with monthly precipitation below 4% of the annual total (Hernandez et al., 1993). The Figure 2b shows the time series of aerosol optical thickness (500 nm) at the Belterra site, near to Santarem, Pará, from 1999 to 2006, showing values significantly lower than Rondônia, but still very high in terms of AOT values.

3. Methods

The set of meteorological and radiation measurements for the RBJ and FLONA-Tapajós sites is based on commercial sensors

coupled to automatic weather stations installed on the towers. Meteorological measurements were averaged to 30 min during the study period. At the RBJ site, the total downward solar radiation was measured with the CM21 pyranometer from Kipp & Zonen, while the total downward PAR radiation was measured with a quantum sensor LI-190SZ from LICOR. At the FLONA-Tapajós site the total downward solar radiation was measured with the CM6 thermopile pyranometer from Kipp & Zonen, and total downward PAR radiation was measured with LI-190 from LICOR.

Both sites were equipped with *eddy-correlation systems*, similar to that described by Moncrieff et al. (1997) and Saleska et al. (2003). At the RBJ site the systems is closed-path, composed of a three axis sonic anemometer (Solent 1012R2, Gill Instruments, UK), and a fast response (0.1 s response time) infrared gas analyser (IRGA, LI-6262, LICOR, USA). The air is collected through a Teflon tube of 4 mm internal diameter, 5 m in length, from an inlet near the sonic anemometer to the IRGA instrument, using a membrane air pump at a flow rate of about 7 l min^{-1}. To prevent dust entering the sampling tubing, Teflon filters of 1 μm pore were used. The CO_2 and H_2O mixing ratio analogue signals plus the sonic anemometer data were processes by A/D converters. This signal plus temperature and wind velocities measured by the sonic anemometer were recorded at a rate of 10.4 Hz for later off-line flux calculations. An algorithm was set to compensate the time delay of the IRGA signals and include corrections for instrument response and damping fluctuations, following the methodology described by Moncrieff et al. (1997) and Aubinet et al. (2000). Generally these corrections were small and represent an almost negligible uncertainty factor on the final carbon flux value (Kruijt et al., 2004).

The closed-path turbulent fluxes of CO_2 at the FLONA-Tapajós site were digitized and stored at 4 Hz. Wind and temperature were measured with a three axis sonic anemometer (Campbell Scientific, Logan UT). The CO_2 and H_2O concentrations were measured using an infrared gas analyser (IRGA, LI-6262, LICOR, Lincoln NE). Air was colleted through a Teflon tube of 9.5 mm inner diameter, 75 m in length, from a coarse polyethylene screen inlet 50 cm above the sonic anemometer, drawing 20–24 standard l min^{-1} of the air through the closed-path IRGA. To prevent dust entering the sampling tubing, Teflon filters of 1 μm pore were used. Corrections for time delay of the IRGA signals, including corrections for instrument response and damping of fluctuations trough the IRGA tube were performed.

The AERONET CIMEL sun-photometers have been operated at two sites: the Abracos Hill site, at the Fazenda Nossa Senhora Aparecida (10°45′S and 62°22′W), about 100 km from the RBJ CO_2 flux tower and the Belterra (02°39′S and 54°57′W) site, close to FLONA-Tapajós CO_2 flux tower (3°01′S and 54°58′W). The AERONET sun photometers were close enough of the towers to be representative of the aerosol loading over them, since during the dry season the atmospheric aerosol loading is a regional component, with high concentrations rather uniform over hundreds of kilometres (Andreae et al., 2002; Procopio et al., 2003).

The data analysis performed in this work cover a measurement period from June 28, 2000 to December 31, 2003 at the FLONA-Tapajós site and from January 28, 2000 to December 31, 2001 at the RBJ site.

3.1. Methodology for the quantification of the aerosol loading and cloud cover

In order to quantify the aerosol and cloud effects on the NEE, we calculated the so-called *relative irradiance* (f) (eq. 1) to produce a measurement of the reduction in the total downward solar flux caused by the presence of aerosol particles and clouds in the atmosphere, compared with the clean atmosphere. The 'experimental' f is defined here as the ratio between the total downward solar irradiance measured by the pyranometer, and the total downward solar irradiance that this same pyranometer would be measuring in cloudless conditions and with atmospheric background aerosol loading (defined at AOT = 0.05, that is the average value of the wet season in both sites) (eq. 1). This cloudless solar irradiance with background aerosol condition was calculated with the radiative transfer code Santa Barbara DISORT Atmospheric Radiative Transfer (SBDART) (Ricchiazzi et al., 1998). The aerosol model used in the SBDART calculations was carefully developed with measurements in Amazonia, and was the same as used in Procopio et al. (2003, 2004).

$$f = \frac{S_{\mathrm{MEAS}}[\mathrm{AOT,clouds\ and\ aerosols}]}{S_0[\mathrm{AOT} = 0.05,\mathrm{cloudless}]} \quad (1)$$

In the eq. (1), S_{MEAS} [AOT, clouds and aerosols] is the total downward solar irradiance measured by the pyranometer in actual sky conditions, and S_0 [AOT = 0.05, cloudless] is the total downward solar irradiance that the same pyranometer would be measured for cloudless and background aerosol (AOT = 0.05) condition, calculated from SBDART. From eq. (1), measurements of f performed during cloudless days with background aerosols show relative irradiance equal to 1.0. Increasing aerosol loading and cloud cover makes f approach zero.

3.2. Methodology used to isolate the aerosol effect on the NEE measurements

Aerosols and clouds both affect the surface radiative flux. To observe only the aerosol effect on the solar irradiance flux (computed from 'f'), and consequently on the NEE measurements, the aerosol effect has to be isolated from the cloud effect. Measurements were classified as affected only by aerosols if they

were performed under cloudless condition. AERONET has a very carefully designed algorithm to exclude cloud contamination on the AOT measurements (Holben et al., 1998). Only AERONET level 2.0 data (after cloud screening and recalibration of the CIMEL sun photometer) were used in this study, but the procedure cannot exclude the possibility of a small cloud contamination that could be observed by the pyranometer, but not sensed by the sun photometer. This condition could happens for instance at high solar zenith angles and for azimuth angles. These unscreened clouds can significantly reduce (or slightly increase) the level of total downward solar irradiance measured by the pyranometer for days viewed as cloudless. This effect, called *cloud gap effect*, (Gu et al., 1999), happens because the sunlit area, located in the end of the trajectory of the solar beam, when this travel between `windows' formed by individual clouds, receives the same amount of direct radiation whatever clouds are present outside the direct view. However, the diffuse fraction is increased due to the scattering and reflection of the beam by adjacent clouds, so the name 'cloud gap effect'.

The *cloud gap effect* was observed in the total downward solar irradiance, and consequently on the f measurements, performed at the RBJ and FLONA-Tapajós site. Therefore to identify cloud influence on the solar irradiance and to separate only the aerosol effect on the relative irradiance (f), the aerosol optical model developed by Procopio et al. (2003, 2004) was used. This approach produces the modeled f (named 'f_S') as a function of the AOT in cloudless conditions (eq. 2):

$$f_S = \frac{S_{\mathrm{SIM}}[\mathrm{AOT, cloudless}]}{S_0[\mathrm{AOT} = 0.05, \mathrm{cloudless}]} \tag{2}$$

S_{SIM}[AOT, cloudless] is the value of the modeled total downward solar irradiance that should be measured by the pyranometer in completely cloudless conditions, for any AOT value, and S_0[AOT = 0.05, cloudless] is the solar irradiance modeled for a cloudless and background aerosol (AOT = 0.05) condition. S_{SIM} [AOT, cloudless] and S_0[AOT = 0.05, cloudless] were calculated with the radiative transfer code SBDART (Ricchiazzi et al., 1998). The inputs used in this code to calculate S_{SIM}[AOT, cloudless] were the optical properties of biomass burning aerosol particles (asymmetry parameter, extinction efficiency and single scattering albedo) derived in previous experiments in the Amazonia. It was considered that the atmospheric background conditions have AOT equal to 0.05 at 500 nm wavelength. The solar irradiance was calculated for the solar spectra (0.3–3.8 μm). This procedure provides an expected (modelled) relationship between relative irradiance and AOT.

Our cloud screening algorithm removes measurements of experimental relative irradiance (f (AOT)) outside the range given by the modelled relative irradiance [f_S (AOT)], plus or minus its standard deviation. Basically, we assume that cloud free conditions occur when $f \pm \sigma$ lie within the interval $f_S \pm \sigma_S$ (σ denotes the standard deviation of f or f_S).

3.3. *Quantifying the aerosol and clouds influence on the NEE*

To quantify the magnitude of the influence of aerosols and clouds on the NEE measurements in relation to clear-sky NEE measurements (background aerosols with AOT = 0.05 and cloudless), the following expression was used:

$$\%NEE = \frac{100 \times [NEE(\alpha) - NEE_{\mathrm{CLEAR-SKY}}(\alpha)]}{NEE_{\mathrm{CLEAR-SKY}}(\alpha)}, \tag{3}$$

where $NEE(\alpha)$ is the measurement of the NEE made for actual sky conditions for a solar zenithal angle α, and the $NEE_{\mathrm{CLEAR-SKY}}$ (α) is the measurement of the NEE in clear-sky days (f equal to 1.0 and AOT = 0.05). $NEE_{\mathrm{CLEAR-SKY}}(\alpha)$ is calculated from the relationship between clear-sky NEE and the solar zenithal angle (α) (Fig. 3a for FLONA-Tapajós and Fig. 3b for RBJ). Calculations were done for morning and afternoon clear-sky NEE because there are asymmetries in the data between the morning and afternoon periods. At the RBJ only a

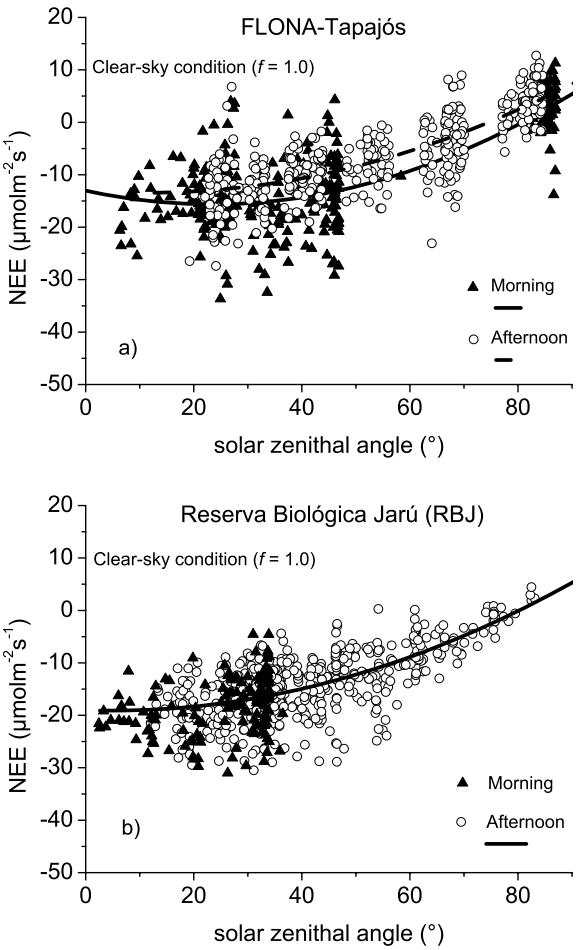

Fig. 3. Relationship between the NEE and solar zenithal angle (α) measurement for clear-sky conditions ($f = 1.0$) at the FLONA-Tapajós (a) and RBJ (b) sites.

few cases of $NEE_{CLEAR-SKY}$ (α) could be obtained for the morning period (Fig. 3b).

4. Results

In the Amazonia most NEE measurements are influenced by clouds, all over the entire year. Even in the dry season, clouds are present most of the time, and precipitation occurs frequently. Hence we first examine the NEE relationship with radiation for a mixture of clouds and aerosols. In this analysis we will study the behaviour of NEE as a function of the relative irradiance (f), for days totally covered by clouds ($f = 0.0$) up to cloudless and background atmospheric aerosol loading days ($f = 1.0$). In the second part of the analysis, the aerosol effect on the NEE will be isolated from the changes at the surface radiation due to clouds, using the cloud screening procedure described in section 3.2.

4.1. The joint effects of clouds and aerosol on the NEE

Figure 4 shows the variability of NEE with the relative irradiance (f) for the FLONA-Tapajós and RBJ site. The data on these two plots were for solar zenithal angle (α) between 25° and 30°. In both sites, the NEE minimum does not occur in clear-sky conditions ($f = 1.0$), but for situations in which there is some aerosols and clouds, that increase the fraction of diffuse radiation.

From eq. (3), the relationship between the %NEE and the relative irradiance was calculated for all solar zenithal angle intervals, from 10° to 70°. The average of the %NEE was calculated in 0.1 bins of the relative irradiance for solar zenithal angle interval of the 20° for the two sites. Figure 5 shows the average relative change in the NEE for relative irradiance range observed, for three intervals of solar zenith angles (α). The data show that at the FLONA-Tapajós, for α between 10° and 30°, the NEE increased by about 15% compared to the clear-sky NEE. At the RBJ, for the same α interval, this increase in the NEE is more pronounced, about 25%. For measurements with $\alpha > 50°$, the two sites have similar patterns of relative changes in the NEE. The increase on the NEE measurements in the presence of aerosols and clouds (in this case mostly clouds) becomes smaller for $\alpha > 50°$ at both sites. In order to obtain the value of the relative irradiance that producing the largest change in the %NEE, we calculated the average of the %NEE in bins of 0.1 (of the relative irradiance) for all measurements with α between 10° and 70°. The result of this calculation is shown in Figure 6, were it is possible to observe that the largest increase on the NEE occurs for the relative irradiances of 0.60–0.75. The maximum increase in the NEE value at the FLONA-Tapajós site was 11% for a relative irradiance value of 0.65. For the RBJ site, the %NEE value increased by 18% for a relative irradiance value of 0.70. Increases in the NEE of 12–18% are very significant, and have important impacts in the Amazonian ecosystem.

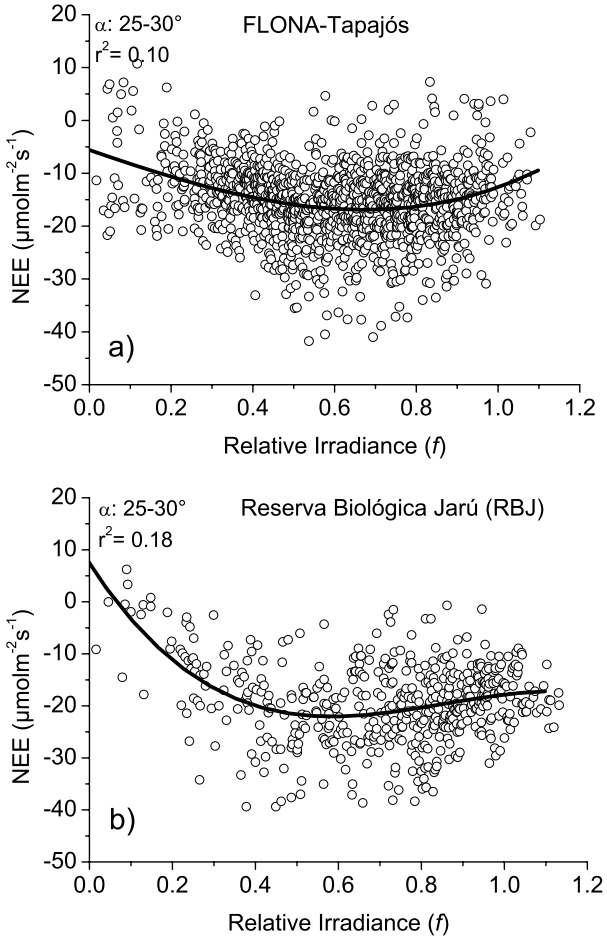

Fig. 4. Variability of NEE with the relative irradiance (f) for the FLONA-Tapajós (a) and RBJ (b) sites for solar zenith angle interval (α) between 25° and 30°.

4.2. The aerosol effect on the NEE measurements

Figure 7 shows the behavior of the relative irradiance (f) as a function of AOT for solar zenithal angle (α) between 20° and 30° after applying the cloud screening process discussed earlier. The reduction of the solar irradiance at the surface due to the radiative effects of aerosols is very large. At the RBJ site, the aerosol loading can cause an instantaneous reduction in the total downward solar irradiance of 192 W m^{-2} for AOT = 1.2, while for AOT = 0.9, there is a reduction of 98 W m^{-2}. At the FLONA-Tapajós site the reduction in the flux is 48 W m^{-2} for AOT = 0.6 at 500 nm. These are very significant reductions in total direct solar flux and there is a strong relationship between relative irradiance and AOT for biomass burning aerosols, as can be observed by the fitted function showed in Figure 7. After cloud screening, it is possible to use either f or AOT for quantifying the amount of particles in the atmosphere, for α between 20° and 30° and AOT values up to 1.4.

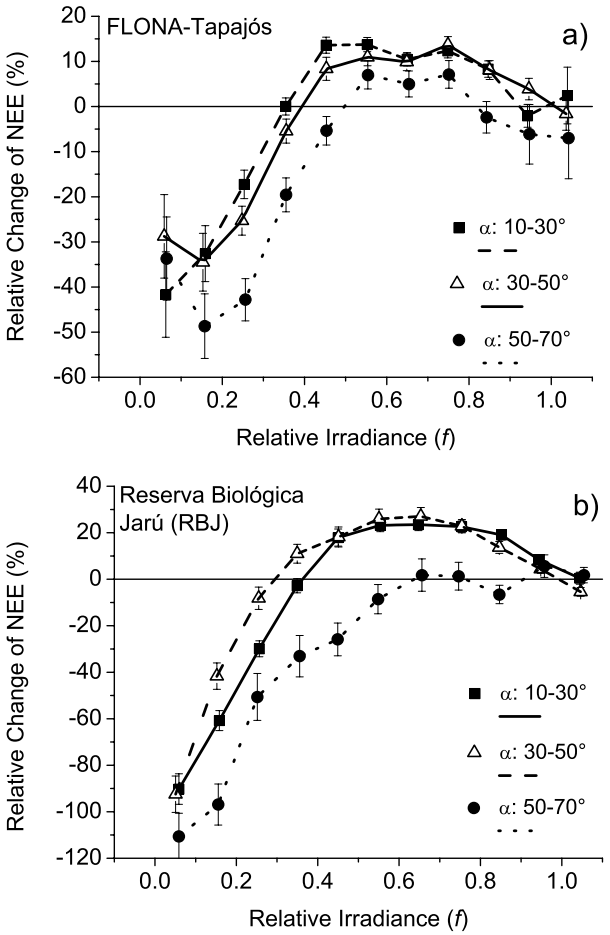

Fig. 5. Relative change of NEE (*%NEE*) as a function of the relative irradiance (f) for three ranges of solar zenithal angle interval (α) for the FLONA-Tapajós (a) and RBJ (b) sites.

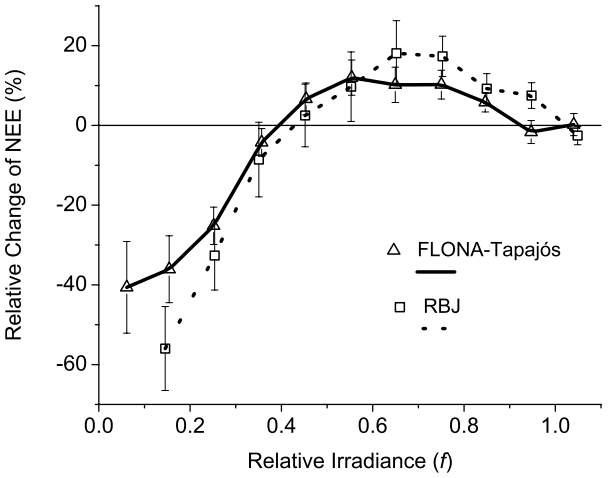

Fig. 6. Relative change of NEE (*%NEE*) as a function of the relative irradiance (f), averaged for all solar zenithal angle intervals (α) (from 10° to 70°). Note that this plot includes clouds and aerosol effects.

Figure 8 shows the relationship between NEE and the relative irradiance (f) for both sites, for α from 20° to 30° after cloud screening process (Section 3.2). It can be observed that with the increase of the amount of aerosol particles in the atmosphere (a reduction of f), the NEE values increase (gets more negative). Similarly for the observation in the case of the predominantly cloud presence, the maximum (more negative) value of the NEE measurements does not occur on clear-sky days ($f = 1.0$ and AOT ~ 0.05), but occurs with relativity high aerosol loading in the atmosphere.

From Figure 9 it was calculated the relative increase in NEE (%NEE) due to the aerosol effects for α between 20° and 30° in both sites. This increase is 8.4% for $f = 0.82$, or AOT $= 0.83$, at the FLONA-Tapajós site. For the RBJ site an increase of 16% was obtained for $f = 0.77$, that corresponds to AOT $= 1.26$.

From relationship between f and %NEE (Fig. 6) and the derived relationship between f and AOT (Fig. 7), it was calculated the AOT value that maximize the %NEE. This value is 1.7 at 500 nm for the FLONA-Tapajós site, with %NEE increase of 11%, and 1.6 at 500 nm for the RBJ site, with %NEE increase of 18%. For larger atmospheric aerosols loadings, NEE is reduced significantly in both sites due to the reduction in the total downward radiation. For values of AOT larger than 2.7 at the RBJ site, for example, NEE approaches to zero.

Figure 10 shows the behavior of the CO_2 flux as a function of the total downward PAR radiation for clear-sky days ($f = 1.0$ and AOT ~ 0.05) and for days with the influence of aerosols and clouds ($f < 1.0$), for FLONA-Tapajós (Fig. 10a) and RBJ (Fig. 10b) sites. It can be observed a large scattering of NEE versus PAR for conditions with aerosols and clouds. From this plot, it is possible to observe that for the same PAR value, 1400 μmol m^{-2} s^{-1}, for example, the NEE measurements are larger (more negative) for days loaded by aerosol and clouds if compared to NEE clear-sky measurements.

5. Possible factors controlling CO_2 fluxes

The presence of aerosol particles and clouds also influences several environmental factors, such as the solar radiation, temperature, humidity, latent heat, precipitation, etc. All these factors have direct or indirect influence on the processes that control the CO_2 exchanges between the forest and the atmosphere. Many authors have pointed out that the radiation use efficiency (RUE) by the forest canopy is larger for the diffuse fraction of the PAR radiation as compared with its direct fraction (Gu et al., 1999, 2001, 2002; Roderick et al., 2001). There is a compensation effect in the carbon uptake through of the increase of the diffuse PAR compared to the decrease of the direct PAR. The analyses presented in this work shows that the FLONA-Tapajós and RBJ sites demonstrate a greater photosynthetic efficiency in cloudy and aerosol-loaded days, as compared to clear-sky days (Fig. 10a and b).

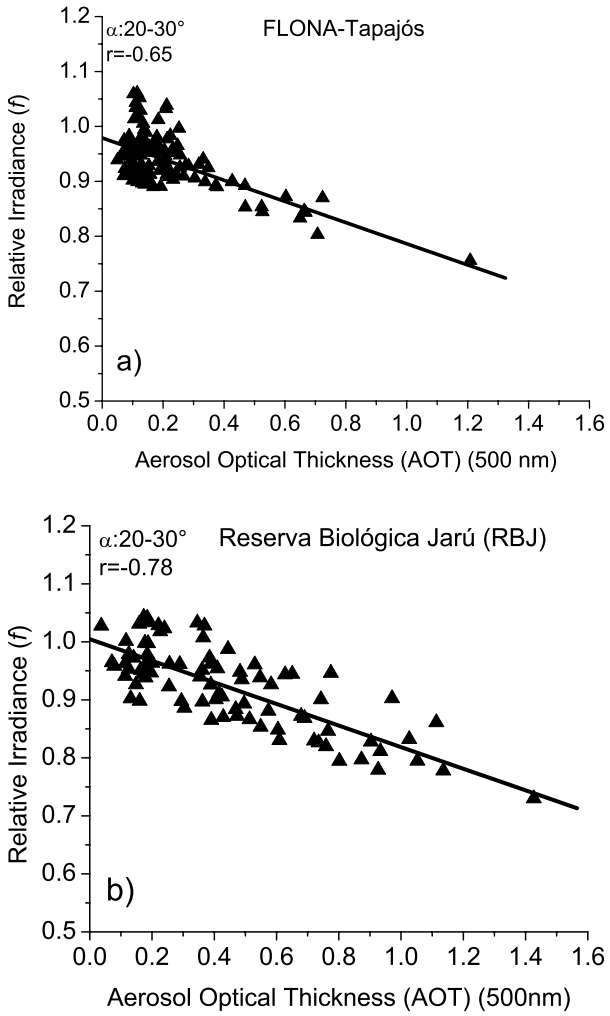

Fig. 7. Relative irradiance (f) as a function of AOT at the FLONA-Tapajós (a) and RBJ (b) sites, for solar zenithal angle (α) between 20° and 30°. The regressions are statistically significant.

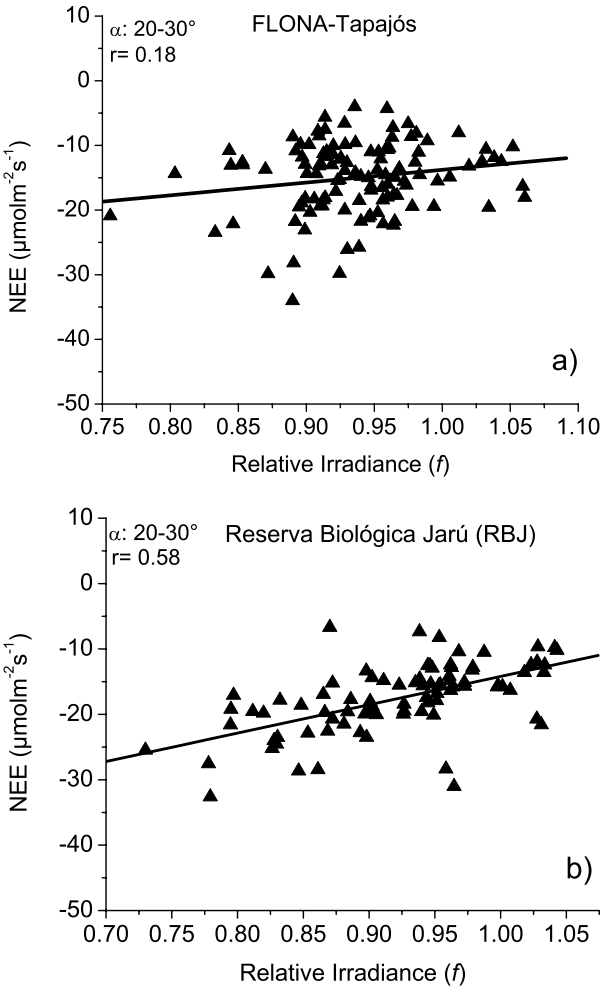

Fig. 8. Aerosols effects on NEE: relative irradiance (f) reduction versus NEE measurements at the FLONA-Tapajós (a) and RBJ (b) sites.

Certainly radiation is not the only factor controlling photosynthesis, and there are other environmental variables that influence the CO_2 fluxes. Surface temperature that is known to affect the photosynthetic rate was found to be significant in affecting CO_2 fluxes. In general, temperature is an important driver in the process of leaf and soil respiration. It is well documented that biomass burning aerosols and clouds cause a reduction of the surface temperature (Schafer et al., 2002a,b; Procopio et al., 2004). In this work, it was possible to observe only the combined effect of all variables on the NEE. It is not possible to separate the radiation changes from temperature or other variables in the NEE values. Another factor that can increase the photosynthesis of the forest canopy is the growth of the relative humidity with the increase of particles and clouds in the atmosphere (Gu et al., 1999; Niyogi et al., 2004). The effect of changes in relative humidity is also difficult to separate from the radiation effects.

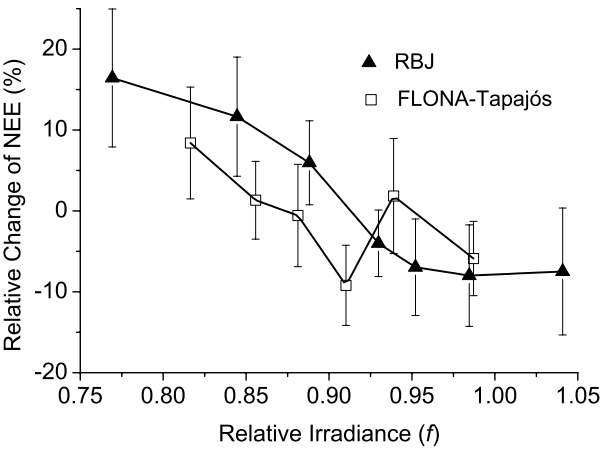

Fig. 9. Relative change of NEE (*%NEE*) due to biomass burning aerosol loading: calculations for solar zenithal angle (α) between 20° and 30°.

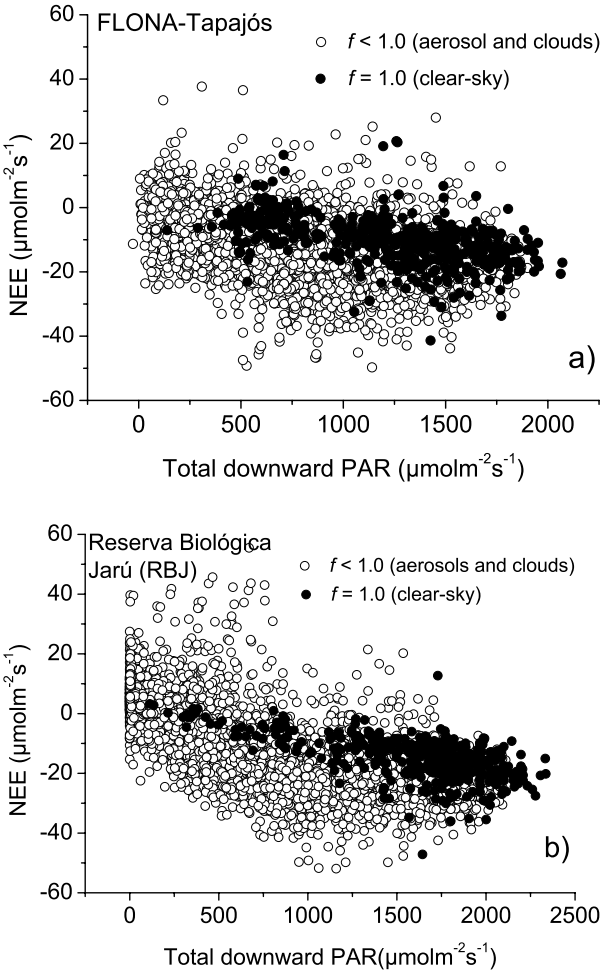

Fig. 10. NEE as a function of total downward PAR radiation for measurements between the 10:00 and 16:00 hr, for the FLONA-Tapajós (a) and RBJ (b) sites.

The aerosol effects on NEE are strong for large areas in Amazonia, and also occur for areas outside the Amazon region, as can be seen in Figure 11. In this MODIS image, a huge smoke plume from biomass burning emissions on September 16, 2004 cover large areas with very high AOT for Amazonia, Southern Brazil, as well as Paraguay, Bolivia, Peru, Venezuela and other countries on South America. Evidently NEE will be affected across the South American continent, and similarly in Africa, Southeast Asia and other regions were biomass burning is an important atmospheric driver.

6. Conclusions

The effect of aerosols and clouds on the CO_2 flux for two sites in Amazonia was observed and quantified. Using sun photometer data from the AERONET network, very high AOT was observed for large areas due to biomass burning emissions, with AOT of 3–4 at 500 nm observed in Rondônia (RBJ site) and values of 1.2–1.6 observed in Santarem (FLONA-Tapajós site). This high aerosol loading and the cloud cover have important impacts on the assimilation of carbon by the Amazonian forest in areas impacted by biomass burning, due to the change in the amount of solar radiation on the ground and due to the increase in the diffuse to direct solar radiation ratio.

At the FLONA-Tapajós site, the average value of the change in NEE is 11% for a level of total radiation of 65% of clear-sky irradiance. For the RBJ site, the increase in NEE is about 18% for a level of total radiation reduction of 70% of clear-sky irradiance.

We also isolated the aerosol effects from cloud effects. It was observed that the relative increase in NEE (%NEE) by the aerosol effect alone is 8.4% for an AOT value of 0.83 at the FLONA-Tapajós site, and 16% for an AOT value of 1.26 at the RBJ site. It was also calculated that the AOT value that maximize the %NEE value is 1.7 at 500 nm for the FLONA-Tapajós site, and 1.6 at 500 nm for the RBJ site. For larger atmospheric aerosols loadings, NEE is reduced significantly due to the reduction in the total radiation. These numbers show that for these two forest ecosystems, clear skies do not provide the ideal environmental condition for the maximum of carbon uptake, and aerosols and clouds actually enhance forest carbon uptake, depending on the atmospheric loading. This is attributed to the increase in the diffuse to direct solar radiation ratio in the forest canopy. Data from both sites showed that as atmospheric aerosol loading and cloudiness increase, several important environmental factors such as temperature and humidity also change. The surface temperature have values significantly reduced due to the clouds and aerosol presence. In this work it was not possible to separate the effects of changes in the solar radiation from changes in the surface temperature and humidity associated with high levels of aerosol particles from biomass burning.

In view of the large aerosol loading for about 4 months and over large areas in Amazonia, the effects of aerosols on the carbon uptake by the Amazonian forest is very significant. The effects observed in Amazonia are certainly also present in tropical forests of Africa and Southeast Asia, because of the similar biomass burning conditions and type of forest. Aerosol particles from biomass burning affect the global carbon budget and a quantification in a global scale could bring an important extra component to the global carbon cycle.

7. Acknowledgments

We thank the large number of researchers, students and technicians contributing to LBA science, from keeping up the continuous tower operation. Also a large number of researchers are contributing to the integration of disciplines that characterizes LBA. We thank MCT and CNPq for the Millennium Institute financial support and CAPES for the master degree scholarship to Paulo Henrique Fernandes de Oliveira. We also thank the LBA-ECO

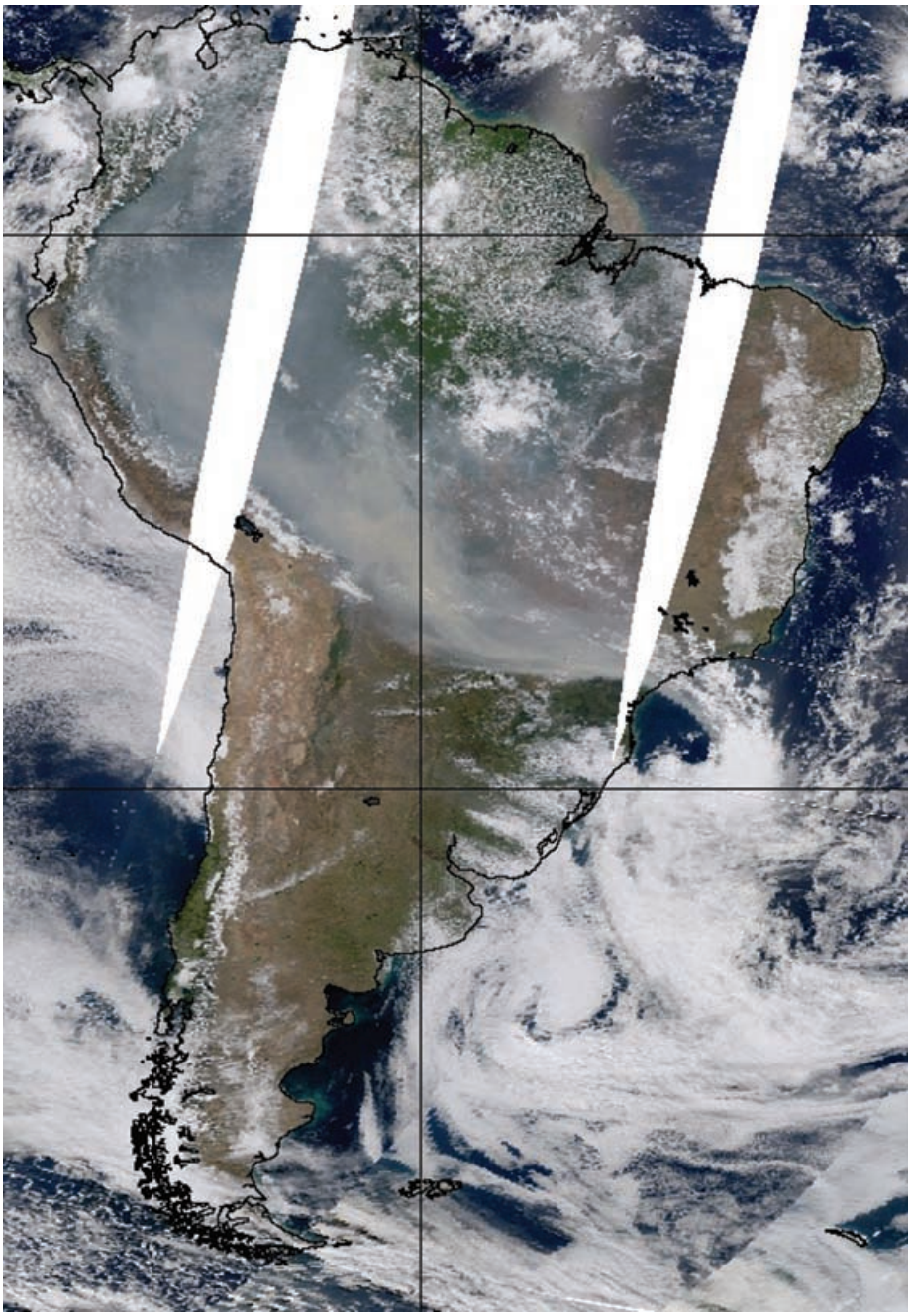

Fig. 11. Large smoke plume from biomass burning emissions on September 16, 2004, measured by MODIS covering large areas with very high AOT for Amazonia, and a large area of South America.

project from NASA for the support of the AERONET network operations.

References

Andreae, M. O., Rosenfeld, D., Artaxo, P., Costa, A. A., Frank, G. P. and co-authors. 2004. Smoking rain clouds over the Amazon. *Science* **303**, 1337–1342.

Andreae, M. O., Artaxo, P., Brandão, C., Carswell, F. E., Ciccioli, P. and co-authors. 2002. Biogeochemical cycling of carbon, water, energy, trace gases, and aerosols in Amazonia: The LBA-EUSTACH experiments. *J. Geophys. Res.* **107**(D20), 8066–8091.

Artaxo, P., Fernandes, E. T., Martins, J. V., Yamasoe, M. A., Hobbs, P. V. and co-authors. 1998. Large-scale aerosol source apportionment in Amazonia. *J. Geophys. Res.* **103**(D24), 31837–31848.

Artaxo, P., Martins, J. V., Yamasoe, M. A., Procopio, A. S., Pauliquevis, T. M. and co-authors. 2002. Physical and chemical properties of aerosols in the wet and dry season in Rondônia, Amazonia. *J. Geophys. Res.* **107**(D20), 8081–8095.

Aubinet, M., Grelle, A., Ibrom, A., Rannik, U., Moncrieff, J. and co-authors. 2000. Estimates of the annual net carbon and water exchange of European forests: the EUROFLUX methodology. *Adv. Ecol. Res.* **30**, 113–175.

Baldocchi, D. D. 1997. Measuring and modelling carbon dioxide and water vapour exchange over a temperate broad-leaved forest during the 1995 summer drought. *Plant, Cell Environ*. **20**, 1108–1122.

Eck, T. F., Holben, B. N., Slutsker, I. and Setzer, A. 1998. Measurements of irradiance attenuation and estimation of aerosol single scattering albedo for biomass burning aerosols in Amazonia. *J. Geophys. Res.* **103**(D24), 31865–31878.

Fan, S., Goulden, M. L., Munger, J. W., Daube, B. C., Bakwin, P. S. and co-authors. 1995. Environmental controls on the photosynthesis and respiration of a boreal lichen woodland: a growing season of whole-ecosystem exchange measurements by eddy correlation. *Oecologia* **102**, 443–452.

Fan, S., Gloor, M., Mahlman, J., Pacala, S., Sarmiento, J. and co-authors. 1998. A large terrestrial carbon sink in North America implied by atmospheric and oceanic carbon dioxide data and models. *Science* **282**, 442–446.

Fearnside, P. M. 1996. Amazonian deforestation and global warming: carbon stocks in vegetation replacing Brazil's Amazon forest. *Forest Ecol. Manag.* **80**, 21–34.

Field, C. B., Behrenfeld, M. J., Randerson, J. T. and Falkowski, P. 1998. Primary production of the biosphere: integrating terrestrial and oceanic components. *Science* **281**, 237–240.

Grace, J., Lloyd, J., McIntyre, J., Miranda, A. C., Meir, P. and co-authors. 1995a. Carbon dioxide uptake by an undisturbed tropical rain forest in Southwest Amazonia, 1992 to 1993. *Science* **270**, 778–780.

Grace, J., Lloyd, J., McIntyre, J., Miranda, A. C., Meir, P. and co-authors. 1995b. Fluxes of carbon dioxide and water vapour over an undisturbed tropical forest in south-west Amazonia. *Global Change Biol.* **1**, 1–12.

Grace, J., Malhi, Y., Lloyd, J., McIntyre, J., Miranda, A. C. and co-authors. 1996. The use of eddy covariance to infer the net carbon dioxide uptake of Brazilian rain forest. *Global Change Biol.* **2**, 209–217.

Gu, L., Fuentes, J. D., Shugart, H. H., Staebler, R. M. and Black, T. A. 1999. Responses of net ecosystem exchange of carbon dioxide to changes in cloudiness: Results from two North American deciduous forests. *J. Geophys. Res.* **104**(D24), 31421–31434.

Gu, L., Fuentes, J. D., Garstang, M., Silva, J. T., Heitz, R. and co-authors. 2001. Cloud modulation of surface solar irradiance at a pasture site in southern Brazil. *Agric. Forest Meteorol.* **106**, 117–129.

Gu, L., Baldocchi, D. D., Verma, S. B., Black, T. A., Vesala, T. and co-authors. 2002. Advantages of diffuse radiation for terrestrial ecosystem productivity. *J. Geophys. Res.* **107**(D6), 4050–4073.

Gu, L., Baldocchi, D. D., Wofsy, S. C., Munger, J. W., Michalsky, J. J. and co-authors. 2003. Response of a deciduous forest to the Mont Pinatubo eruption: enhanced photosynthesis. *Science* **299**, 2035–2038.

Hernadez, P., Shimabukuro, Y. E., Lee, D. C. L., Santos, C. P., Almeida, R. R. 1993. *Projeto de Inventário florestal na Floresta Nacional do Tapajós*. São José dos Campos, INPE, 126 p.

Holben, B. N., Eck, T. F., Slutsker, I., Tanré, D., Buis, J. P. and co-authors. 1998. AERONET-A federated instrument network and data archive for aerosol characterization. *Remote Sens. Environ.* **66**, 1–16.

Hollinger, D. Y., Kelliher, F. M., Byers, J. N., Hunt, J. E., McSeveny, T. M. and co-authors. 1994. Carbon dioxide exchange between an undisturbed old-growth temperate forest and the atmosphere. *Ecology* **75**, 134–150.

Houghton, R. A., Skole, D. L., Nobre, C. A., Hackler, J. L., Lawrence, K. T. and co-authors. 2000. Annual fluxes of carbon from deforestation and regrowth in the Brazilian Amazon. *Nature* **403**, 301–304.

INPE (Instituto Nacional de Pesquisas Espaciais). 2004. *Desflorestamento 1998–2004*. INPE, São José dos Campos, São Paulo, Brazil.

Keller, M., Rocha, H. R., Trumbore, S. and Kruijt, B. 2001. Investigating the carbon cycle of the Amazon forests. *IGBP Newslett.* **45**, 15– 19.

Kaufman, Y. J. and Koren, I. 2006. Smoke and pollution aerosol effect on cloud cover. *Science* **313**, 655–658.

Koren, I., Kaufman, Y. J., Remer, L. A. and Martins, J. V. 2004. Measurement of the effect of Amazon smoke on inhibition of cloud formation. *Science* **303**, 1342–1345.

Kruijt, B., Elbers, J. A., von Randow, C., Araujo, A. C., Oliveira, P. J. and co-authors. 2004. The robustness eddy correlation fluxes for Amazon rain of forest conditions. *Ecol. Appl.* **14**(4), 101–113.

Malhi, Y., Nobre, A. D., Grace, J., Kruijt, B., Pereira, M. G. P. and co-authors. 1998. Carbon dioxide transfer over a Central Amazonian rain forest. *J. Geophys. Res.* **103**(D24), 31593–31612.

Marengo, J. A. and Nobre, C. A. 2001. General characteristics and variability of climate in the Amazon Basin and its links to the global climate system. In: *The Biogeochemistry of the Amazon Basin* (eds. McClain, M. E., Victoria, R. L., Richey, J. E.). Oxford University Press, New York, 17–41.

Melillo, J. M., Houghton, R. A., Kicklighter, D. W. and McGuire, A. D. 1996. Tropical deforestation and the global carbon budget. *Ann. Rev. Energy Environ.* **21**, 293–310.

Moncrieff, J. B., Massheder, J. M., de Bruin, H., Elbers, J., Friborg, T. and co-authors. 1997. A system to measure surface fluxes of momentum, sensible heat, water vapour and carbon dioxide. *J. Hydrol.* **188**, 589–611.

Niyogi, D., Chang, H., Saxena, V. K., Holt, T., Alapaty, K., Booker, F. and co-authors. 2004. Direct observations of the effects of aerosol loading on net ecosystem CO_2 exchanges over different landscapes. *Geophys. Res. Lett.* **31**, 20506–20511.

Ometto, J. P., Nobre, A. D., Rocha, H. R., Artaxo, P. and Martinelli, L. A. 2005. Amazonia and the modern carbon cycle: lessons learned. *Oecologia* **143**(4), 483–500.

Price, D. T. and Black, T. A. 1990. Effects of short-term variation in weather on diurnal canopy CO_2 flux and evapotranspiration of a juvenile Douglas-Fir stand. *Agric. Forest Meteor.* **50**, 139–158.

Procopio, A. S., Artaxo, P., Kaufman, Y. J., Remer, L. A., Schafer, J. S. and co-authors. 2004. Multiyear analysis of Amazonian biomass burning smoke radiative forcing of climate. *Geophys. Res. Lett.* **31**, 3108–3112.

Procopio, A. S., Remer, L. A., Artaxo, P., Kaufman, Y. J. and Holben, B. N. 2003. Modeled spectral optical properties for smoke aerosols in Amazonia. *Geophys. Res. Lett.* **30**(24), 2265–2270.

Ricchiazzi, P., Yang, S., Gautier, C. and Sowle, D. 1998. SBDART: A research and teaching software tool for plane-parallel radiative transfer in the earth's atmosphere. *Bull. Am. Meteorol. Soc.* **79**, 2101–2114.

Roderick, M. L., Farquhar, G. D., Berry, S. L. and Noble, I. R. 2001. On the direct effect of clouds and atmospheric particles on the productivity and structure of vegetation. *Oecologia* **129**, 21–30.

Saleska, S. R., Miller, S. D., Matross, D. M., Goulden, M. L., Wofsy, S. C. and co-authors. 2003. Carbon in Amazon forests: unexpected seasonal fluxes and disturbance-induced losses. *Science* **302**, 1554–1557.

Schafer, J. S., Holben, B. N., Eck, T. F., Yamasoe, M. A. and Artaxo, P. 2002a. Atmospheric effects on insolation in the Brazilian Amazon: Observed modification of solar radiation by clouds and smoke and derived single scatter albedo of fire aerosols. *J. Geophys. Res.* **107**(D20), 8074–8089.

Schafer, J. S., Eck, T. F., Holben, B. N., Artaxo, P., Yamasoe, M. A. and Procopio, A. S. 2002b. Observed reductions of total irradiance by biomass-burning aerosols in the Brazilian Amazon and Zambian Savanna. *Geophys Res. Lett.* **29**(17), 1823–1826.

Schimel, D. S. 1995. Terrestrial ecosystems and the carbon-cycle. *Global Change Biol.* **1**, 77–91.

Schimel, D. S., House, J. I., Hibbard, K. A., Bousquet, P., Ciais, P. and co-authors. 2001. Recent patterns and mechanisms of carbon exchange by terrestrial ecosystems. *Nature* **414**, 169–172.

Silva Dias, M. A. F., Rutledge, S., Kabat, P., Silva Dias, P. L., Nobre, C. and co-authors. 2002. Clouds and rain processes in a biosphere-atmosphere interaction context in the Amazon Region. *J. Geophys. Res.* **107**(D20), 8072–8092.

Tans, P. P. and White, J. W. C. 1998. The global carbon-cycle: in balance, with a little help from the plants. *Science* **281**, 183–184.

von Randow, C., Sá, L. D. A., Prasad, G. S. S. D., Manzi, A. O., Arlino, P. R. A. and co-authors. 2002. Scale variability of atmospheric surface layer fluxes of energy and carbon over a tropical rain forest in south-west Amazonia 1. Diurnal conditions. *J. Geophys. Res.* **107**(D20), 8062–8074.